# COMPARISON OF 1D AND 2D CSR MODELS WITH APPLICATION TO THE FERMI@ELETTRA BUNCH COMPRESSORS*

G. Bassi†, BNL, Upton, NY 11973-5000, USA.
J. A. Ellison, K. Heinemann, University of New Mexico, Albuquerque, NM 87131, USA

*Abstract*

We compare our 2D mean field (Vlasov-Maxwell) treatment of coherent synchrotron radiation (CSR) effects with 1D approximations of the CSR force which are commonly implemented in CSR codes. In our model we track particles in 4D phase space and calculate 2D forces [1]. The major cost in our calculation is the computation of the 2D force. To speed up the computation and improve 1D models we also investigate approximations to our exact 2D force. As an application, we present numerical results for the Fermi@Elettra first bunch compressor with the configuration described in [1].

## CSR MODELS FOR BUNCH COMPRESSORS

In this paper we discuss and compare 1D and 2D models to study CSR effects in bunch compressors. In Fig. 1 we plot the reference curve (blue curve) for a four dipole (regions in gray) chicane bunch compressor in the $(Z, X)$-plane of the lab system. The parameters are for the Fermi@Elettra first bunch compressor (see Table 1).

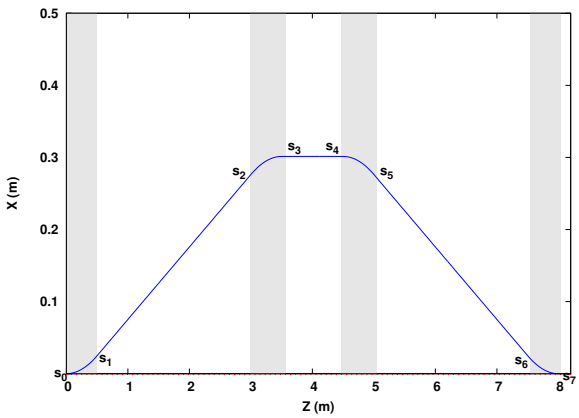


Figure 1: First bunch compressor of Fermi@Elettra. The curve in blue is the reference curve in laboratory system. The regions in gray represent the magnets.

### *Self-consistent 2D model*

We summarize the two-dimensional mean field treatment of CSR effects discussed in [1]. We use Frenet-Serret coordinates with respect to the reference curve and have, in addition to the lab system, two coordinate systems, one with $u = ct$ as independent variable where path length $s$ is a dependent variable and one coordinate system where $s$ is the independent variable and $u$ is a dependent variable. Following [2] we call the former "beam system 1" and the latter "beam system". In [1] we used the terminology "beam frame" instead of "beam system" but that term can be confused with "inertial frame". The equations of motion in the beam system are

$$z' = -\kappa(s)x\ , \quad x' = p_x\ ,$$
$$p_z' = \frac{q}{P_r c}[\mathbf{t}(s) + p_x \mathbf{n}(s)] \cdot \mathbf{E}_{\parallel}(\hat{\mathbf{R}}, s)\ ,$$
$$p_x' = \kappa(s) p_z + \frac{q}{P_r c}\left[\mathbf{n}(s) \cdot \mathbf{E}_{\parallel}(\hat{\mathbf{R}}, s) - c B_Y(\hat{\mathbf{R}}, s)\right]\ , \quad (1)$$

where $' = d/ds$ and $\hat{\mathbf{R}} = \mathbf{R}_r(s) + M(s)\mathbf{r}$. Here $\mathbf{R}_r(s) = (Z_r(s) X_r(s))^T$ gives the reference curve in the lab system, $\mathbf{t} = (Z_r', X_r')^T$, $\mathbf{n} = (-X_r', Z_r')^T$, $M = [\mathbf{t}, \mathbf{n}]$, $\mathbf{r} = (z, x)^T$ and $P_r$ is the momentum of the reference particle. These are eqs. (27) of [1] and can be derived from eqs. (78) of [2] using a slowly varying approximation.

The self-fields are retarded solutions of Maxwell's equations, given by

$$\begin{pmatrix} \mathbf{E}_{\parallel} \\ B_Y \end{pmatrix}(\mathbf{R}, u) = -\frac{1}{4\pi}\int_{-\infty}^{u}\int_{-\pi}^{\pi} \mathbf{S}(\tilde{\mathbf{R}}(\theta, v), v) d\theta dv,$$

where $\tilde{\mathbf{R}}(\theta, v) = \mathbf{R} + (u - v)\mathbf{e}(\theta)$ and $\mathbf{S}$ is the lab system source term related to the charge/current density $\rho_L, \mathbf{J_L}$ in the lab system. These densities are determined from the phase space density $f_B$ in the beam system [2]. For more details see [1, 2].

### *1D model*

Here we consider the model developed by Saldin et al. [3] and Stupakov et al [4]. We distinguish two cases.

Table 1: Chicane and Beam Parameters at First Dipole

| Parameter | Symbol | Value | Unit |
|---|---|---|---|
| Energy reference particle | $E_r$ | 233 | MeV |
| Peak current | I | 120 | A |
| Bunch charge | Q | 1 | nC |
| Norm. transverse emittance | $\gamma\epsilon_0$ | 1 | $\mu$m |
| Alpha function | $\alpha_0$ | 0 | |
| Beta function | $\beta_0$ | 10 | m |
| Linear energy chirp | h | -12.6 | 1/m |
| Uncorrelated energy spread | $\sigma_E$ | 2 | KeV |
| Momentum compaction | $R_{56}$ | 0.057 | m |
| Radius of curvature | $R$ | 5 | m |
| Magnetic length | $L_b$ | 0.5 | m |
| Distance 1st-2nd, 3rd-4th bend | $L_1$ | 2.5 | m |
| Distance 2rd-3nd bend | $L_2$ | 1 | m |

* Work supported by DOE under DE-FG-99ER41104 and DOE contract DE-AC02-98CH10886
† gbassi@bnl.gov

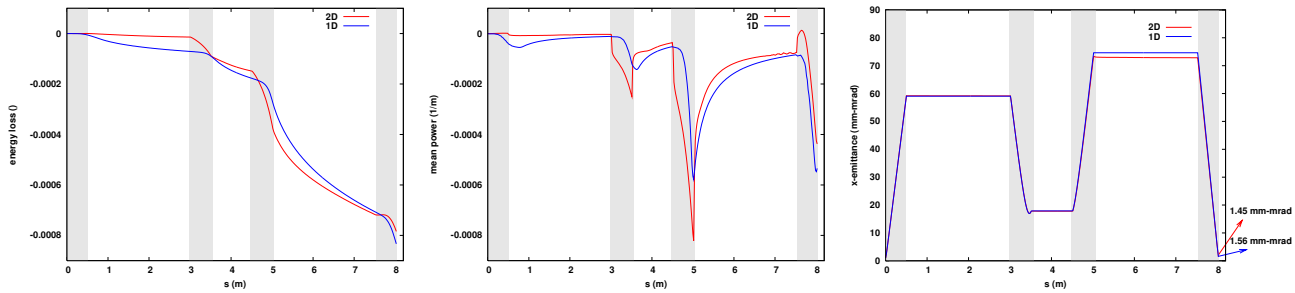


Figure 2: Comparison of the 2D model [1] and the 1D model [3], [4]. Left: mean energy loss. Center: mean power. Right: x-emittance.

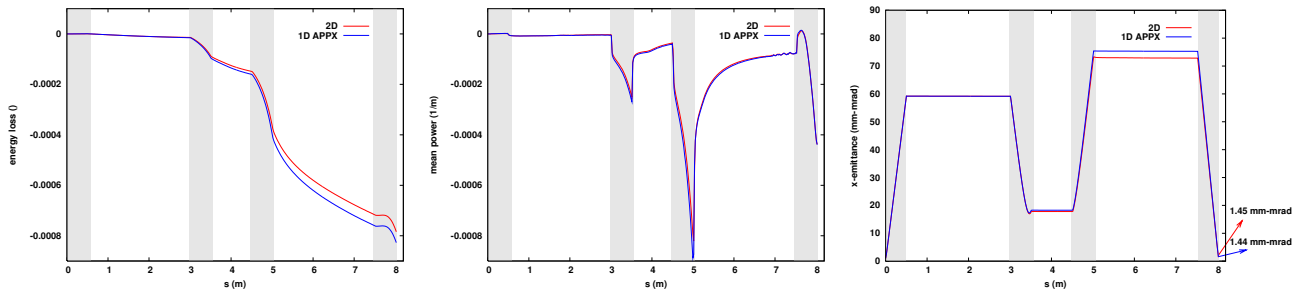


Figure 3: Comparison of the 2D model [1] and the 1D approximation scheme discussed in the paper. Left: mean energy loss. Center: mean power. Right: x-emittance.

When the particle beam is inside the magnet, the CSR force is formula (87) of [3], which is equivalent to formula (5) + (6) of [4]. When the beam is in the drift, an explicit formula (formula (10) + (15) of [4]) has been obtained by Stupakov et al. based on Saldin's formalism [3]. Apparently that formalism is developed in our beam system 1. In appendix A we show how to write down the formulae in the beam system using the results derived in [2]. The equations of motion corresponding to eq. (1) are

$$z' = -\kappa(s)x\ , \qquad p_z' = G_B(z,s)\ ,$$
$$x' = p_x\ , \qquad p_x' = \kappa(s)p_z\ . \tag{2}$$

If the beam is inside the magnets, i.e. $s_i \le s \le s_{i+1}$ for $i = 0, 2, 4, 6$ (see Fig. 1), we have

$$G_B(z,s) = -\frac{4r_0N}{\gamma_r R\phi}\Big[\lambda_B\Big(z-\frac{R\phi^3}{24},s\Big) - \lambda_B\Big(z-\frac{R\phi^3}{6},s\Big)\Big]$$
$$-\frac{2r_0N}{\gamma_r(3R^2)^{1/3}}\int_{z-R\phi^3/24}^{z}\frac{1}{(z-z')^{1/3}}\frac{\partial}{\partial z'}\lambda_B(z',s)dz', \tag{3}$$

where $\phi = (s - s_i)/R$, $R$ is the radius of curvature of the magnets, $r_0 = q^2/4\pi\varepsilon_0 m_e c^2$ the classical radius of the electron, $\gamma_r$ the Lorentz factor of the reference particle, $N$ the number of electrons in the beam and $\lambda_B := \int dp_z dp_x dx f_B$ is the longitudinal density in the beam system.

If the beam is outside the magnets, i.e. $s_i \le s \le s_{i+1}$ for $i = 1, 3, 5, 7$ (see Fig. 1), we have

$$G_B(z,s) = -\frac{4r_0N}{\gamma_r R}\Big[\frac{\lambda_B(z-\Delta s_{\max},s)}{\phi_m+2\hat{s}}$$
$$-\frac{1}{\phi_m+2\hat{s}}\lambda_B\Big(z-\frac{R}{6}\phi_m^2(\phi_m+3\hat{s}),s\Big)$$
$$+\int_{z-\Delta s_{\max}}^{z}\frac{1}{\psi(z')+2\hat{s}}\frac{\partial}{\partial z'}\lambda_B(z',s)dz'\Big], \tag{4}$$

where

$$\phi_m = \frac{s_1}{R}, \quad \hat{s} = \frac{s-s_i}{R}, \quad \Delta s_{\max} = \frac{R\phi_m^3}{24}\frac{\phi_m+4\hat{s}}{\phi_m+\hat{s}}, \tag{5}$$

and $\psi(z')$ is obtained from the equation

$$z - z' = \frac{R\psi^3}{24}\frac{\psi+4\hat{s}}{\psi+\hat{s}}. \tag{6}$$

Note that SI units are used.

## NUMERICAL RESULTS FOR FERMI@ELETTRA BC1

We apply the 2D and 1D models to the Fermi@Elettra first bunch compressor (BC1). Numerical results with the 2D model are discussed in [1] where the microbunching instability is analyzed. The phase space distribution at entrance to the bunch compressor is taken to be Gaussian. In Fig. 2 we compare mean energy loss, mean power (mean value of $p_z'$) and transverse emittance. Even though eqs. (1) and (2) are quite different, both in form and method of derivation, the agreement between the 2D and 1D model is good. The 1D model does underestimate the CSR force in the second and third magnet, as shown in Fig. 2 (center). We are working to understand this agreement by a

detailed comparison of eq. (1) and (2). The final transverse emittance (Fig. 2, right) is 1.45$\mu$m with the 2D model and 1.56$\mu$m with the 1D model. A good agreement of 1D and 2D CSR models with detailed measurements of the CSR-induced energy loss and transverse emittance growth has been found recently in [5]. This may lead to the conclusion that 1D models are reliable and that there is no need for 2D models. Despite these results, we believe that a more accurate comparison should be performed to validate 1D models in the study of effects such as the microbunching instability. We are planning to apply the 1D model to the study of the microbunching instability in the Fermi@Elettra BC1 and compare the results obtained with the 2D model of [1].

We conclude with the discussion of a 1D approximation to our 2D model. We have discovered that the beam system spatial density is almost stationary in the $(\tilde{z},\tilde{x})$ coordinates given by eq. (38) of [1]. Our 1D approximation takes $\tilde{x} = 0$ and the $\hat{\mathbf{R}}$ in eq. (1) becomes $\hat{\mathbf{R}} = \mathbf{R}_r(s)+M(s)(1+hR_{56}(s), hD(s))^T\tilde{z}$. The accuracy of the scheme is shown in Fig. 3. The approximation to the mean power and transverse emittance is excellent. The final value of the transverse emittance is 1.44$\mu$m, to be compared with 1.56$\mu$m of the exact 2D model. The calculation is considerably faster than the 2D calculation as it reduces the computational cost by a factor proportional to the number of grid points in $\tilde{x}$. We believe this works because of a weak dependence of $F_{z1}$ on its second argument for fixed values of the first, as illustrated in Figs. 4 and 5 where we have plotted $F_{z1}(\tilde{z},\tilde{x},s) = (q/P_rc)\mathbf{E}_{||}(\hat{\mathbf{R}},s)\cdot\mathbf{t}(s)$ in $(\hat{z},\hat{x})$ coordinates that put the 5 sigma range of the tilde variables on the square $[-1,1]^2$. This weak dependence is satisfied to good approximation where the CSR force has its maximum strength, namely inside the magnets, with the worst case scenario for $s = 5$m illustrated by Fig. 4. A more detailed discussion, together with an analysis of the relation between the CSR forces in eq. (1) and (2), will be presented in a forthcoming paper [6]. We are also planning to validate this approximation scheme against the exact 2D model in the study of the microbunching instability [1]. On our agenda is also the comparison of the 1D and 2D models with the LCLS bunch compressors [5] where measurements have been done in a strong CSR regime.

## APPENDIX: SALDIN'S FORMULA WITH S AS INDEPENDENT VARIABLE

We now show how to derive formula (4) with $s$ as independent variable from Saldin's formula (87) of [3] that has $u = ct$ as independent variable. We first write the right-hand side of Saldin's formula (87) in the form

$$G_1(s,u) = -A\Big[B(s)\Big(\lambda_1(s-s_L,u)-\lambda_1(s-4s_L,u)\Big) + \int_{s-s_L}^{s}\frac{1}{(s-s')^{1/3}}\frac{\partial}{\partial s'}\lambda_1(s',u)ds'\Big], \quad (7)$$

where $A = 2r_0N/(\gamma_r(3R^2)^{1/3})$, $B(s) = s_L^{-1/3}$ and $s_L = R\phi^3/24$. Using the density transformation between lab and beam system $\lambda_1(s,u) = \lambda_B(s-\beta_ru,s)$ [2] and assuming the following slowly varying approximation (SVA)

$$\lambda_B(z,s+\Delta)\simeq\lambda_B(z,s), \quad \Delta\approx\sigma\ (\sigma = \text{bunch length})$$

it follows that

$$G_B(z,s) = G_1(s,u=\frac{s-z}{\beta_r}) = -A\Big[B(s)\Big(\lambda_B(z-s_L,s)-\lambda_B(z-4s_L,s)\Big) + \int_{s-s_L}^{s}\frac{1}{(s-s')^{1/3}}\frac{\partial}{\partial s'}\lambda_B(s'-s+z,s')ds'\Big]. \quad (8)$$

Using again the SVA and changing integration variable $z' = s'-s+z$ we have

$$G_B(z,s) = -A\Big[B(s)\Big(\lambda_B(z-s_L,s)-\lambda_B(z-4s_L,s)\Big) + \int_{z-s_L}^{z}\frac{1}{(z-z')^{1/3}}\frac{\partial}{\partial z'}\lambda_B(z',s)dz'\Big], \quad (9)$$

which is equivalent to eq (3). A similar argument leads from formula (10) + (15) of [4] to eq. (4).

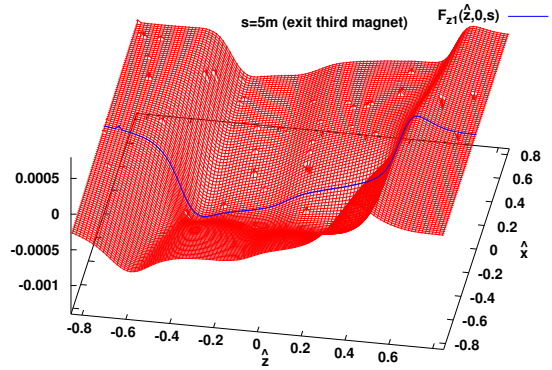


Figure 4: Plot of $F_{z1}(\tilde{z},\tilde{x},s)$ in normalized coordinates at s=5m (exit third magnet). The 1D approximation scheme uses $F_{z1}(\tilde{z},0,s)$ (blue line).

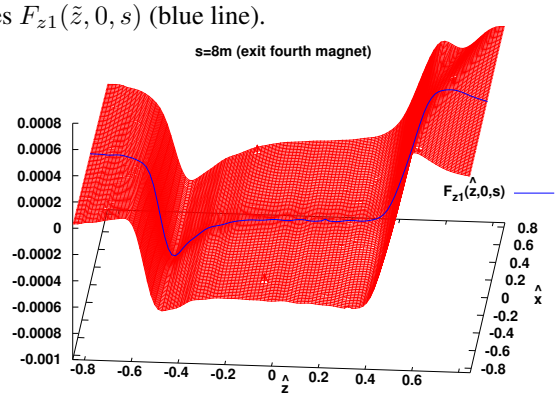


Figure 5: The same as in Fig. 4 for s=8m (end of chicane).

## REFERENCES

[1] Phys. Rev. ST Accel. Beams **12**, 080704 (2009).
[2] Phys. Rev. ST Accel. Beams **13**, 104403 (2010).
[3] NIMA **398** (1997).
[4] Paper WEPRI029, Proceedings of EPAC 2002, Paris, France.
[5] Phys. Rev. ST Accel. Beams **12**, 030704 (2009).
[6] In preparation.